(11) R. E. D. McClung, *J. Chem. Phys.*, **51**, 3842 (1969).
(12) R. E. D. McClung, *J. Chem. Phys.*, **57**, 5478 (1972).
(13) R. E. D. McClung, *Adv. Mol. Relax. Int. Proc.*, **10**, 83 (1977).
(14) K. J. Shin, D. S. Chung and B. S. Kim, *J. Chem. Phys.*, **77**, 5852 (1982).
(15) A. Abragam, "The Principles of Nuclear Magnetism," Oxford Univ. Press, 1961.
(16) See, for example, J. O. Hirschfelder, C. F. Curtiss, and R. B. Bird, "Molecular Theory of Gases and Liquids," John Wiley & Sons, New York, 1954.

Tunnel Effects in the H + D_2 and D + H_2 Reactions

Jongbaik Ree, Young Seek Lee, In Joon Oh and Taikyue Ree†

Department of Chemistry, Korea Advanced Institute of Science and Technology, P.O. Box 150, Chongyangni, Seoul 131, Korea *(Received October 12, 1982)*

We considered the tunneling effect on the rate constants calculated from transition-state theory for the H + D_2 and D + H_2 reactions. A method for evaluating the important parameter E_c (potential barrier height) was proposed. A tunnel-effect correction factor (TECF) $\Gamma_t \exp\theta_t$ was estimated from experimental data, and compared with the corresponding values obtained from many theoretical methods. According to our results, the tunneling effect cannot be negligible around 800°K where the TECF value is ca. 0.8 whereas the factor approaches to unity at T>2400°K where the tunneling completely disappears. In addition to the above fact, we also found that the TECF for the D+H_2 reaction is greater than that of the H+D_2 reaction in agreement with Garrett and Truhlar's result. In contrast to our result, however, Shavitt found that the order is reversed, *i. e.*, TECF for (D+H_2) is greater than that for (H+D_2). We discussed about the Shavitt's result.

1. Introduction

A quantum mechanical tunneling effect is very important for reactions involving light atoms and molecules, and the neglect of this factor often causes the rate constants from activated complex theory to be too small.[1-5] In the past two decades, noteworthy progress in the computation of tunneling factor has been made.[1-12]

The first quantum correction was derived by Wigner in 1932,[7] and this simplified model had been used widely for its computational simplicity. Wigner's quantum correction, however, is justified only when the tunneling correction is small, and the conditions for validity of Wigner's assumptions are seldom to be satisfied. A theoretically more justifiable way is to include tunneling effects involving an exact quantum mechanical transmission probability through a given potential barrier.[1] In simple cases, it is sufficient to use a parabolic or Eckart-type barrier, since for these barriers the transmission probability G(W) can be analytically computed.[1,3,4] But, for more complicated cases, one must calculate the transmission probability numerically to obtain the tunneling factor Γ_t because of the complexity of the potential barrier. Thus, effective potential energy barriers are often employed, the most commonly used models are the CVE (conservation of vibrational energy) barrier[10] and the 'vibrationally adiabatic' (VA) barrier.[10-12] In the latter, there are the MEPVA (minimum energy path vibrationally adiabatic) barrier and the MCPVA (Marcus-Coltrin path vibrationally adiabatic) barrier. These two VA methods and the CVE method are very well compared in Figure 1 of ref. 5. The VA methods, however, are not used in the present paper.

Meanwhile, many *ab initio* and semiempirical methods have been used for constructing the potential energy surface of H_3.[13-18] The most accurate three-dimensional potential energy surface for H_3 is the one obtained by Siegbahn and Liu (SL)[18] by using a configuration interaction method. Among other *ab initio* calculations for obtaining the potential energy surface, however, the method used by Shavitt, Stevens, Minn and Karplus (SSMK)[17] is easier than the SL method, and it yields results of fairly high accuracy. Thus, the SSMK surface has been most widely used, we also employ the SSMK potential energy barrier in the present work.

In view of the experiment, the H+H_2 reaction and its isotopic reactions[3,19-22] are not particularly simple to study. Especially, at low temperatures, the experimental procedure is difficult, as a result, the experimental kinetic data are very rare and also are of poor accuracy. This situation has been partly improved at least by the ESR method of Westenberg and de Hass,[21] and Mitchell and LeRoy.[22]

Finally, it should be pointed out that if we calculate the rate constants k' theoretically using the barrier heights (E_c) which were computed by *ab initio* or semiempirical methods, the theoretical values of k' are smaller than the experimental data. Thus, the theoretical barrier height E_c has been adjusted to give agreement with the high-temperature part of the available experimental data.[1]

In this paper we consider the following two reactions which have been studied by many authors[19-22] theoretically and

experimentally:

$$H+D_2 \longrightarrow HD+D \quad (1)$$

and

$$D+H_2 \longrightarrow DH+H \quad (2)$$

we have evaluated the tunnel-effect correction factor (TECF) $\Gamma_t \exp\theta_t [\theta_t = d\ln\Gamma_t/d\ln T]$ for the above hydrogen reactions by using the experimental rate data. This factor will be called the "empirical tunnel-effect correction factor." We have also calculated the theoretical TECF, where Γ_t and θ_t were theoretically calculated by using several methods proposed by other authors. The empirical and theoretical TECF's are compared in this paper. For this purpose, a simple and satisfactory method for evaluating the theoretical E_c has been proposed in this paper. We expect that this method will also be used in many other studies.

2. Theory

(1) The Rate Equation for Hydrogen Atom and Molecule Reactions

As well-known, the Arrhenius rate equation is

$$k' = A\exp(-E_a/RT) \quad (3)$$

where k' is the rate constant, E_a is the activation energy and A is the frequency factor.

The general form of the theoretical equation for k' based on transition state theory is[23]

$$k' = B(T)\exp(-E_c/RT) \quad (4)$$

where, $B(T)$ for $H+H_2$ reaction and its isotopic reactions is written by the following equation for a linear activated complex:

$$B(T) = \frac{S^*\Gamma_t h^2}{(2\pi)^{3/2}(kT)^{1/2}}\left(\frac{M^*}{M_a M_m}\right)^{3/2}\frac{I^+}{I_m}\frac{\sinh\frac{1}{2}\beta\nu_m}{4\sinh\frac{1}{2}\beta\nu_s^+\left(\sinh\frac{1}{2}\beta\nu_b^+\right)^2} \quad (5)$$

in this expression, the subscripts a and m refer to the reactant atom and reactant molecule, respectively, the superscript $+$ indicates the activated complex, M is the mass, I is the moment of inertia, S^* is the statistical factor, Γ_t is the tunneling factor, $\beta = h/kT$ (where k is Boltzmann's constant) and ν is the vibrational frequency, the subscripts s and ν refer to the symmetric stretching and bending modes, respectively.

From Eqs. (3) and (4), one obtains the following equation:[23]

$$E_a = E_c + \Theta RT \quad (6)$$

where Θ is defined by $d\ln B(T)/d\ln T$, and is represented by the following equation for reactions (1) and (2):

$$\Theta = \frac{1}{2}(f^* - f_{\text{reactants}}) + \sum_{i=1}^{3}\left[\left(\frac{u_i^+}{2}\right)\coth\left(\frac{u_i^+}{2}\right)-1\right] - \left[\left(\frac{u_m}{2}\right)\coth\left(\frac{u_m}{2}\right)-1\right]+\theta_t$$

$$= \frac{1}{2}\left[-1+u_s^+\coth\left(\frac{u_s^+}{2}\right)+2u_b^+\coth\left(\frac{u_b^+}{2}\right) - u_m\coth\left(\frac{u_m}{2}\right)\right]+\theta_t \quad (7)$$

In Eq. (7), f indicates the number of degrees of freedom of a molecule or an atom including the reaction mode, $u_i = h\nu_i/kT$, and

$$\theta_t = \frac{d\ln\Gamma_t}{d\ln T} \quad (8)$$

By the definition of the activation energy in terms of experimental observables, it is given by

$$E_a = -R\frac{d\ln k'}{d(1/T)} \quad (9)$$

Thus, if we obtain E_a from Eq. (9) with available experimental data, and substitute this E_a into Eq. (6), we can calculate the potential barrier height E_c since the factor Θ is calculable as shown in the following. The term θ_t in Θ [Eq. (7)] will be considered in detail in Part III.

(2) Evaluation of the TECF ($\Gamma_t \exp\theta_t$) from Experimental Rate Data

By substituting Eq. (6) into Eq. (4), one obtains

$$k' = B(T)\exp\left(\Theta - \frac{E_a}{RT}\right) \quad (10)$$

The substitution of Eq. (7) into Eq. (10) yields:

$$k' = B(T)\exp\left[\frac{1}{2}\left\{-1+u_s^+\coth\left(\frac{u_s^+}{2}\right)+2u_b^+\coth\left(\frac{u_b^+}{2}\right) - u_m\coth\left(\frac{u_m}{2}\right)\right\}+\theta_t\right]\times\exp(-E_a/RT) \quad (11)$$

By rearranging Eq. (11), in which B(T) has been substituted by Eq. (5), one obtains the following equation:

$$\Gamma_t e^{\theta_t} = k'\exp\left(\frac{E_a}{RT}\right) \times\left[\frac{S^* h^2}{(2\pi)^{3/2}(kT)^{1/2}}\left(\frac{M^+}{M_a M_m}\right)^{3/2}\frac{I^+}{I_m}\times\frac{\sinh\frac{1}{2}\beta\nu_m}{4\sinh\frac{1}{2}\beta\nu_s^+\left(\sinh\frac{1}{2}\beta\nu_b^+\right)^2}\right]^{-1} \times\exp\left[\frac{-1}{2}\left\{-1+u_s^+\coth\left(\frac{u_s^+}{2}\right)+2u_b^+\coth\left(\frac{u_b^+}{2}\right)-u_m\coth\left(\frac{u_m}{2}\right)\right\}\right] \quad (12)$$

thus, if we know E_a, the experimental rate constant k' and the frequencies (u_s^+, u_b^+, u_m), we can evaluate the TECF from Eq. (12). The $\Gamma_t \exp\theta_t$ thus obtained is defined as the "empirical tunnel-effect correction factor."

3. Calculations

(1) Estimation of the Activation Energy

In order to obtain the activation energy E_a from observed rate constants k' we performed a nonlinear regression,[24]

$$y = A + B\exp(Cx) \quad (13)$$

where y corresponds to $\ln k'$, and x equals $1/T$. Now, by comparing Eq. (9) with Eq. (13), one obtains easily

$$E_a = -R \cdot y' = -1.987\, B\, C \exp(Cx) \tag{14}$$

(2) The Evaluation the Barrier Height E_c

Let $V(s)$ be the effective potential energy barrier along the reaction coordinate s, and let V_{max} be the potential maximum at $s=s_{max}$ (saddle point). Then the quantum mechanical tunneling factor, Γ_t, on the reaction coordinate motion at temperature T is defined by the following equation:[1]

$$\Gamma_t = \frac{\int_0^{\infty} G(W) \exp(-W/RT)\, dW}{\int_{V_{max}}^{\infty} \exp(-W/RT)\, dW} = \left(\frac{1}{RT}\right) \exp\left(\frac{V_{max}}{RT}\right) \int_0^{\infty} G(W) \exp\left(-\frac{W}{RT}\right) dW \tag{15}$$

where, W is the energy of the reactant system, and $G(W)$ is the quantum mechanical transmission probability. From Eqs. (8) and (15), θ_t is given by

$$\theta_t = -1 - \frac{E_c}{RT} + \frac{1}{RT} \frac{\int_0^{\infty} G(W) \cdot W \cdot \exp(-W/RT)\, dW}{\int_0^{\infty} G(W) \exp(-W/RT)\, dW} \tag{16}$$

where $G(W)$ was assumed to be temperature independent, and E_c equals V_{max} in Eq. (15).

Substitute Eq. (16) into Eq. (7), and then substitute the quantity θ thus obtained into Eq. (6). By these procedure, one obtains the following equation:

$$\frac{\bar{W}}{RT} = \frac{3}{2} + \frac{E_a}{RT} - \frac{1}{2}\left[u_s^{\ddagger} \coth\left(\frac{u_s^{\ddagger}}{2}\right) + 2u_b^{\ddagger} \coth\left(\frac{u_b^{\ddagger}}{2}\right) - u_m \coth\left(\frac{u_m}{2}\right)\right] \tag{17}$$

where,

$$\bar{W} = \frac{\int_0^{\infty} G(W)\, W \exp(-W/RT)\, dW}{\int_0^{\infty} G(W) \exp(-W/RT)\, dW} \tag{18}$$

Now, we must know $G(W)$ to evaluate $\bar{W}$ from which the potential barrier height E_c is obtained as described below.

For example, we consider the Eckart potential energy barrier. The symmetric form of the Eckart barrier is written as[6]

$$V(s) = E_c \operatorname{sech}^2(\pi s/l) \tag{19}$$

In Eq. (19), l is the width parameter, and s is the coordinate along the reaction path. By using the $V(s)$ given by Eq. (19), and by solving the Schrödinger equation, the transmission probability $G(W)$ is obtained as given by the following equation:[1]

$$G(W) = \frac{\cosh(4\pi\alpha) - 1}{\cosh(4\pi\alpha) + \cosh(2\pi\delta)} \tag{20}$$

where

$$\alpha = \frac{1}{4} D (W/E_c)^{1/2} \tag{21}$$

$$\delta = \frac{1}{2}(D^2 - 1)^{1/2} \tag{22}$$

and

$$D = \frac{4E_c}{h|\nu_u|} \tag{23}$$

Next, we consider how to determine E_c. The latter is obtained from Eq. (17), but it is not explicitly involved in Eq. (17). We see, however, that the term $\bar{W}$ in Eq. (17) is given by Eq. (18) in which G(W) is expressed by Eqs. (20) to (23), the factors α, δ and D being the functions of E_c. [See Eqs.(20) to (23)]

In Eq. (17), E_a is obtainable from experiment,[19-22] and the frequency factors $u_s^{\ddagger}$, $u_b^{\ddagger}$ and u_m are obtainable from the SSMK paper.[17] Thus, the right-hand-side term of Eq. (17) is completely calculable. Therefore the problem how to obtain E_c is concentrated to the problem for finding $\bar{W}$ which satisfies Eq. (17), $\bar{W}$ being a function of E_c through Eqs. (18) and (20) to (23). An iterative method is employed for finding E_c in this procedure.

(3) Computation of the Tunneling Factor Γ_t

(i) The Eckart Potentials. As already mentioned, the Eckart I potential is described by Eq. (19) with the corresponding transmission coefficient $G(W)$ [Eq. (20)]. The Eckart III potential[4] has been referred frequently in the literature. According to this potential, the barrier height becomes $E_c = 4.005$ kcal/mole. Concerning the Eckart II potential, we shall not explain since it has not been used in our paper.

(ii) Shavitt Barrier. When $G(W)$ is an analytical form such as of Eq. (20), we can compute Γ_t easily from Eq. (15) by numerical integration. However, when it is not the case, the computation of Γ_t is not an easy task. Thus, Gårrett and Truhlar[5(b)] adapted $G^s(W)$ which is a semiclassical approximation to the transmission probability $G(W)$, and is expressed by the following equation:

$$G^s(W) = \{1 + \exp[2\theta(W)]\}^{-1} \tag{24a}$$

where

$$\theta(W) = \hbar^{-1} \int_{s_<}^{s_>} ds \{2u[V(s) - W]\}^{1/2},\ W < E_c \tag{24b}$$

where $s_<$ and $s_>$ the lower and upper classical turning points, respectively. The potential V^s(s) in Eq. (24b) is expressed by

$$V^s(s) = b_1 \operatorname{sech}^2(b_3 S^2) + b_2 \exp(-b_4 S^2) + (B - b_1 - b_2 \exp(-4b_4 S^2) \tag{25}$$

where B is the barrier height, E_c. This barrier was obtained from the *SSMK* potential energy surface by fitting the potential $V(s)$ by using Eq. (25), and was named the "Shavitt barrier" by Truhlar and Kuppermann,[10] the values of the parameters are

$$b_1 = 0.0850\, eV,\ b_2 = 0.2520\, eV,\ b_3 = 0.25602\,(\text{bohr})^{-2},\ b_4 = 0.89044\,(\text{bohr})^{-2}. \tag{26}$$

Garrett and Truhlar[5(b)] made a program (named KAPPAS) which is very economical and has a sufficient accuracy. This program, which was modified in part by us, uses the $G^s(W)$ [Eq.(24a) with (24b)], $V^s(s)$ [Eq.(25)] and the tunneling factor Γ_t^s which is given by Eq. (27):[5(b)]

$$\Gamma_t^s = 1 + 2\beta \int_{W_0}^{E_c} dW\, G^s(W) \sinh[\beta(E_c - W)] \tag{27}$$

where W_0 is the threshold energy, and it is zero for a symmetrical barrier. In the present study by assuming $W_0=0$, we have calculated Γ_t^s by using the modified KAPPAS program in which the program for obtaining $\theta(W)$ by Eq. (24b) is also included.

(iii) CVE Barrier. Truhlar and Kuppermann[10] suggested that the minimum-energy path of interest in transition state theory is the path of seteepest descent in the normal mode coordinate space extending from the transition state (saddle point) to the reactants configuration. They determined this path for the SSMK surface by using a 29-parameter fit, then expressed the important part for tunneling as a function of a reaction coordinate s by using Eq. (25). (Refer to Table II in ref. 10.) For this path, the parametric values are:

$$b_1=0.1129\,eV,\quad b_2=0.2294\,eV,$$
$$b_3=0.30855\,(\text{bohr})^{-2},\quad b_4=1.11123\,(\text{bohr})^{-2}. \qquad (28)$$

This reaction path is called the CVE barrier.[10] We have used the latter for computing $G^s(W)$ from Eqs. (24a) and (24b), and have computed Γ_t^s from Eq. (27) by using the modified KAPPAS program.

(iv) Statistical Factor. The statistical factor s^+ has been studied by Schlag, Bishop, Laidler *et al.*,[25-30] but a complete resolution has not been given yet. In our study, we use the method proposed by Laidler *et al.*[28,29] According to the latter, $s^+=2$ for reactions (1) and (2).

4. Results

(1) Activation Energy

In Table 1 are shown the observed rate constants[20,21] and the activation energies E_a for the $H+D_2$ reqction. The experimental data of $\ln k'$ vs. $1/T$ fitted by Eq. (13), then the E_a were obtained by applying Eq. (14). In Table 2, the values of k' and E_a are shown for the $D+H_2$ reaction.[21,22] One notes from Tables 1 and 2 that E_a increases with temperature. This is due to the decrease in the tunnel effect.

(2) Potential Energy Barrier Height E_c.

We performed the procedure for finding E_c described in the Calculations [III. (2)]. In the calculation of the right-hand-side term of Eq. (17), the vibrational frequency data listed in Table 3 were used. In Table 4, are shown the potential energy barrier heights E_c, which were evaluated by our method proposed in the Calculations [III. (2)]. and are compared with the literature value.[1]

The first column in Table 4, gives the potential barriers which were used for obtaining E_c. For example, for obtaining $E_c=9.529$ kcal/mole (the first row), the Eckart I potential barrier was used, *i. e.*, G(W) given by Eqs. (19) to (23) was used, and $\bar{W}$ in Eq. (17) was computed from Eq. (18). For Shavitt barrier, $G^s(W)$ is given by Eq. (24a) with (24b) and $V^s(s)$ is given by Eq. (25) with (26); $\bar{W}$ was calculated from Eq. (18) as in the above case, and $E_c=9.491$ kcal/mole was obtained by an iterative method. For the CVE potential barrier, a similar method as in the Shavitt barrier was used, *i. e.*, G^s(W) is given by Eq. (24a) with (24b), but $V^s(s)$ is given by Eq. (25) with (28). For obtaining $E_c=9.595$ kcal/mole, the same procedure as in the above cases was used.

From Table 4, one notes that the Eckart III potential with $E_c=4.005$ kcal/mole is unreasonably small, although it was proposed by Shavitt to explain the rate constants of the $H+D_2$ and $D+H_2$ reactions [see the Discussion].

(3) Tunneling Factor Γ_t and its Logarithmic Temperature Coefficient θ_t.

In Table 5 are shown the Γ_t data (unparenthesized) calculated by various methods shown on the head line. The second column gives the Γ_t value calculated from Eq. (15) where $G(W)$ [Eq.(20) with (21) to (23)] was calculated by using the Eckart I potential [Eq. (19)], taking $E_c=9.529$ kcal/mole. The third column was obtained by a similar procedure as above except that for calculating $G(W)$, the Eckart III potential was used, *i. e.*, $E_c=4.005$ kcal/mole. By using the modified KAPPAS program, the fourth and fifth columns were obtained, in the former, the Shavitt potential $V^s(s)$ [Eq.(25) with (26) and E_c (Shavitt)=9.491 kcal/mole], and in the latter, the CVE potential $V^s(s)$ [Eq. (25) with (28) and E_c (CVE)=9.595 kcal/mole] were used for calculating $G^s(W)$ from Eq. (24a) with (24b); and the factor Γ_t^s was calculated from Eq. (27) for both Shavitt and *CVE* potentials.

The parenthesized values in Table 5 are the θ_t data which were calculated from Eq. (16) by using the G(W) or $G^s(W)$ for the respective potentials.

(4) The Tunnel-Effect Correction Factor $\Gamma_t \exp\theta_t$.

In Table 6 are listed the values of $\Gamma_t \exp\theta_t$. The values in columns 3 to 6 are the values of $\Gamma_t \exp\theta_t$ obtained from the

TABLE 1: Experimental Rate Constants and Observed Activation Energies for the $H+D_2$ Reaction[a]

Temp.(° K)	k'(cc/mole. sec)	E_a(kcal/mole)[b]	Temp.(° K)	k'(cc/mole. sec)	E_a(kcal/mole)[b]
299	1.56(7)[c]	7.788	420.6	7.044(8)[d]	8.663
327	3.77(7)[c]	8.037	421.0	6.966(8)[c]	8.665
346	7.60(7)[c]	8.187	439.1	9.795(8)[c]	8.759
368.0	2.101(8)[d]	8.344	439.7	1.013(9)[d]	8.762
368.2	2.167(8)[d]	8.346	440	1.07(9)[c]	8.763
368.4	1.940(8)[d]	8.347	449.1	1.216(9)[d]	8.808
368.8	2.019(8)[d]	8.350	449.9	1.335(9)[d]	8.812
386.0	3.246(8)[d]	8.462	467.7	1.728(9)[d]	8.894
404.4	4.833(8)[d]	8.572	549	8.70(9)[c]	9.210
404.8	4.918(8)[d]	8.574	745	8.70(10)[c]	9.709

[a] In this table the numerals inside the parentheses indicate the exponent to base 10. [b] Calculated from Eq. (14) using the experimental rate constants; [c] Reference 21; [d] Reference 20.

TABLE 2: Experimental Rate Constants and Observed Activation Energies for the D+H$_2$ Reaction[a]

Temp.(° K)	k'(cc/mole. sec)	E_a(kcal/mole)[b]	Temp.(° K)	k'(cc/mole. sec)	E_a(kcal/mole)[b]
167	5.78(4)[c]	5.095	269	5.25(7)[c]	6.325
178	2.21(5)[c]	5.278	272	5.17(7)[c]	6.350
184	5.23(5)[c]	5.371	274	7.30(7)[d]	6.366
188	3.80(5)[c]	5.430	276	7.06(7)[c]	6.382
195	8.10(5)[c]	5.530	281	9.00(7)[c]	6.421
196	1.12(6)[c]	5.544	291	1.14(8)[c]	6.497
198	8.81(5)[c]	5.571	297	1.61(8)[d]	6.540
206	1.97(6)[c]	5.676	299	1.75(8)[d]	6.554
212	2.32(6)[c]	5.751	305	2.00(8)[c]	6.595
216	2.82(6)[c]	5.799	315	2.94(8)[c]	6.660
227	6.95(6)[c]	5.924	325	4.56(8)[c]	6.723
237	1.28(7)[c]	6.030	337	6.62(8)[c]	6.793
244	1.77(7)[c]	6.100	346	8.25(8)[c]	6.843
247	2.00(7)[c]	6.129	352	9.15(8)[d]	6.876
248	1.95(7)[c]	6.138	438	7.30(9)[d]	7.251
251	1.83(7)[c]	6.166	543	3.60(10)[d]	7.562
252	3.60(7)[d]	6.176	548	3.95(10)[d]	7.574
259	3.01(7)[c]	6.239	745	2.60(11)[d]	7.930
262	3.32(7)[c]	6.265			

[a] In this table, the numerals inside the parentheses indicate the exponent to base 10; [b] Calculated from Eq. (14) using the experimental rate constants; [c] Reference 22; [d] Reference 21.

TABLE 3: Vibrational Quanta, $Nh\nu$ (kcal/mole)[a]

species	$Nh\nu_m$	$Nh\nu_s$	$Nh\nu_b$	$Nh\nu_u$
HH	12.574			
DD	8.894			
HDD		4.979	2.122	3.137i
DHH		4.984	2.660	3.963i

[a] Reference 4.

TABLE 4: The Potential Energy Barrier Height, E_c

Potential Barrier	E_c(kcal/mole)
Eckart I	9.529
Shavitt	9.491
CVE	9.595
Previous work	9.785[a]

[a] Reference 4.

data of Γ_t and θ_t in Table 5. In column 2, the "empirical" values of $\Gamma_t \exp\theta_t$ are given which were calculated from Eq. (12) by the use of experimental k' and E_a in conjunction with the vibrational frequency factors, $u_a^{\pm}$, $u_b^{\pm}$ and u_m (Table 3). [See Theory. (2).]

In Figure 1 are shown the factors $\Gamma_t \exp\theta_t$ against $T(° K)$ for the H+D$_2$ reaction. The factors were calculated by four different ways which are labeled on the curves, and are illustrated in detail in the caption to Figure 1. Except "Eckart I (KAPPAS)," other three methods were already used for calculating Tables 5 and 6. In fact, the curves, Eckart I, Eckart III and CVE, are the reproduction from Table 6. The Eckart I (KAPPAS) curve was obtained by a similar method as in the CVE curve, *i.e.*, Γ_t and θ_t were obtained from Eq. (27) with $G^s(W)$ given by Eqs. (24a) and (24b), but for $V^s(s)$, the Eckart I potential barrier [Eq. (19) with E_c=9.529 kcal/mole] was used. [Note: The factor π/l in Eq. (19) is equal to $\alpha'/2$ where $\alpha'=2.10$.[5(b)] Thus $V^s(s)$ is calculable from Eq. (19) as a function of s.]

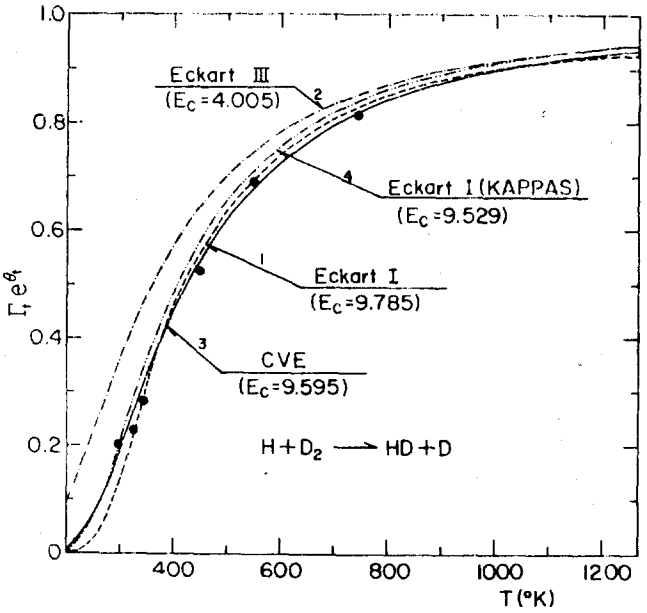

Figure 1. The plots of $\Gamma_t \exp\theta_t$ vs T for the $H+D_2$ reaction. Curve 1: Γ_t and θ_t were obtained from Eqs. (15) and (16), respectively. Where G(W) was obtained from Eqs. (20) to (23) by using Eckart I potential barrier [Eq. (19)] with E_c=9.785 kcal/mole; Curve 2: obtained by same procedure as in curve 1, but with E_c=4.005 kcal/mole; Curve 3: Γ_t and θ_t were obtained from Eq. (27), where $G^s(W)$ was obtained from Eqs. (24a) and (24b) by using the CVE potential barrier [Eq. (25) and (28)] with E_c=9.595 kcal/mole; Curve 4: obtained by the same procedure as in Curve 3, but by using the Eckart I barrier [Eq. (19)] with E_c=9.529 kcal/mole; Dots: Empirical $\Gamma_t \exp\theta_t$; E_c in Figure 1 and following figures are in units of kcal/mole.

In Figure 1, the four calculated $\Gamma_t \exp\theta_t$ curves are com-

TABLE 5: Theoretical Values of Γ_t (or Γ_t') and θ_t for the $H+D_2$ and $D+H_2$ Reactions[a]

Temp.(° K)	Eckart I	Eckart III	Shavitt	CVE
$H+D_2$ Reaction				
299	3.855	3.293	3.100	3.733
	(-3.040)	(-2.214)	(-2.546)	(-2.954)
327	3.024	2.746	2.526	2.944
	(-2.415)	(-1.857)	(-2.046)	(-2.379)
346	2.662	2.486	2.267	2.596
	(-2.100)	(-1.663)	(-1.788)	(-2.081)
440	1.811	1.805	1.631	1.768
	(-1.203)	(-1.049)	(-1.032)	(-1.203)
549	1.466	1.493	1.361	1.432
	(-0.747)	(-0.695)	(-0.637)	(-0.743)
745	1.238	1.269	1.179	1.211
	(-0.402)	(-0.399)	(-0.335)	(-0.391)
$D+H_2$ Reaction				
252	27.244	10.594	3.791	4.758
	(-8.028)	(-4.224)	(-3.096)	(-3.616)
274	14.902	7.632	3.003	3.624
	(-6.428)	(-3.628)	(-2.496)	(-2.922)
297	9.349	5.815	2.503	2.927
	(-5.187)	(-3.130)	(-2.042)	(-2.393)
299	9.032	5.695	2.469	2.881
	(-5.096)	(-3.092)	(-2.009)	)-2.354
	(-5.096)	(-3.092)	(-2.009)	(-2.354)
352	4.588	3.682	1.882	2.096
	(-3.344)	(-2.292)	(-1.364)	(-1.598)
438	2.604	2.437	1.488	1.592
	(-1.977)	(-1.538)	(-0.834)	(-0.976)
543	1.859	1.853	1.290	1.346
	(-1.226)	(-1.045)	(-0.524)	(-0.614)
548	1.839	1.835	1.284	1.339
	(-1.202)	(-1.028)	(-0.514)	(-0.602)
745	1.401	1.439	1.142	1.168
	(-0.636)	(-0.598)	(-0.271)	(-0.316)

[a] Unparenthesized and parenthesizde data are Γ_t (or Γ_t') and θ_t, respectively.

TABLE 6: Tunnel-Effect Correction Factor $\Gamma_t \exp \theta_t$ for the $H+D_2$ and $D+H_2$ Reactions.

Temp (° K)	Empirical	Eckart I	Eckart III	Shavitt	CVE
$H+D_2$ Reaction					
299	0.205	0.184	0.360	0.243	0.195
327	0.230	0.270	0.429	0.372	0.273
346	0.285	0.326	0.471	0.379	0.324
440	0.518	0.544	0.632	0.581	0.531
549	0.692	0.694	0.745	0.719	0.681
745	0.815	0.828	0.851	0.843	0.820
$D+H_2$ Reaction					
252	0.175	0.009	0.155	0.171	0.128
274	0.190	0.024	0.203	0.248	0.195
297	0.228	0.052	0.254	0.325	0.267
299	0.236	0.055	0.259	0.331	0.274
352	0.366	0.162	0.372	0.481	0.424
438	0.598	0.361	0.523	0.646	0.600
543	0.667	0.546	0.652	0.763	0.729
548	0.698	0.553	0.657	0.767	0.733
745	0.831	0.741	0.791	0.872	0.851

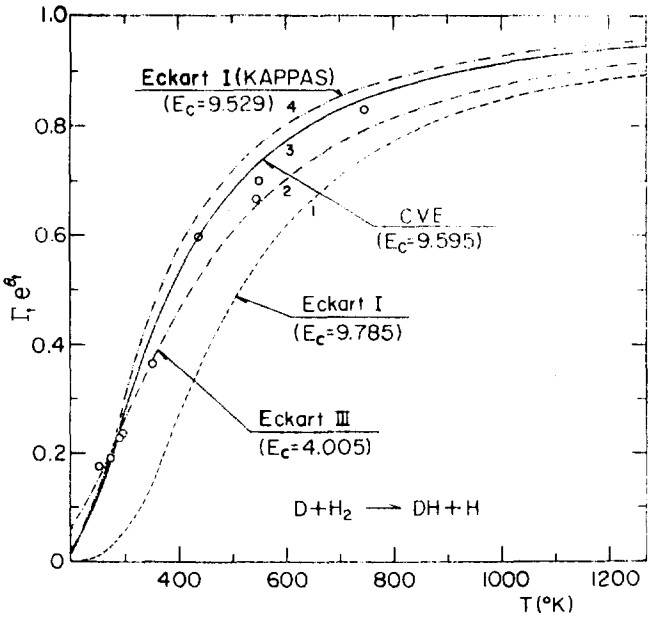

Figure 2. The plots of $\Gamma_t \exp \theta_t$ vs T for the $H+D_2$ reaction. Curves 1, 2, 3 and 4 obtained by the same procedure as described for the corresponding curves in the captions to Figure 1. Circules are the empirical $\Gamma_t \exp \theta_t$.

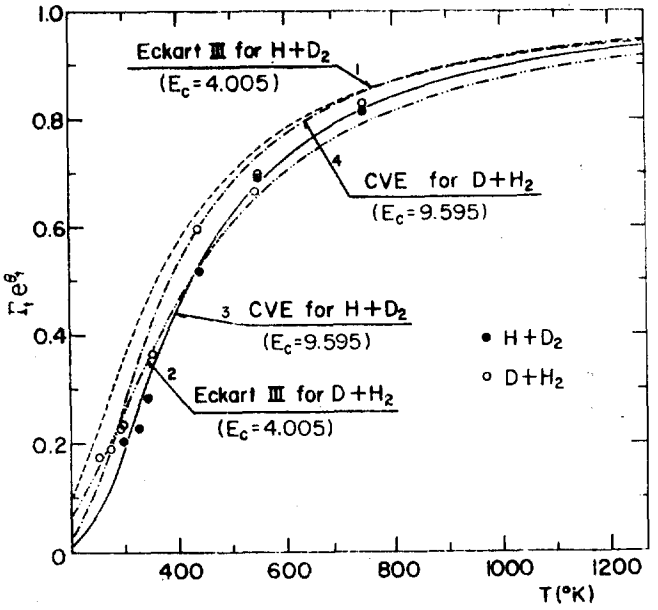

Figure 3. The plots of $\Gamma_t \exp \theta_t$ vs T for the $H+D_2$ and $D+H_2$ reactions. Curve 1 is the replica of curve 2 in Figure 1; Curve 2 is the replica of curve 2 in Figure 2; Curve 3 is the replica of curve 3 in Figure 1; Curve 4 is the replica of curve 3 in Figure 2. Open and filled circles are the empirical $\Gamma_t \exp \theta_t$ of the $D+H_2$ and $H+D_2$ reactions, respectively.

pared with the empirical $\Gamma_t \exp \theta_t$ values (presented by dots) which were calculated from Eq. (12).

In Figure 2, a similar representation as in Figure was done for the $D+H_2$ reaction. The empirical data of $\Gamma_t \exp \theta_t$ are shown by circles in Figure 2. From Figures 1 and 2, one notes that the CVE curves show better agreement with the empircial data.

By using the data of the CVE $\Gamma_t \exp \theta_t$ in Table 6, the TECF values for the $H+D_2$ and $D+H_2$ reactions are compared in Figure 3. A similar comparison is also made with respect those curves calculated by using the Eckart III poten-

tial. Also in Figure 3, the empirical $\Gamma_t \exp\theta_t$ data for the two reactions are shown; the comparison shows that the empirical data for reaction $H+D_2$ (shown by filled circles) are smaller than those for reaction $D+H_2$ (shown by open circles). One also notes that this trend appears in the CVE curves whereas the Eckart III curves show the opposite effect. From this comparison, one may conculude that the Eckart III potential is not realistic.

(5) Calculation of the Rate Constants k'.

In Figure 4 are plotted the data of log k' vs $1/T$ for reactions of $H+D_2$ and $D+H_2$. Curve 1 for both reactions is the theoretical log k' calculated by Shavitt by using Eq. (4) with (5), where E_c=9.785 kcal/mole was used for calculating the exponential factor of k' in Eq. (4) whereas the Γ_t in B(T) [Eq. (5)] was computed from Eqs. (15) and (20) to (23) by using the Eckart III barrier E_c=4.005 kcal/mole. The inconsistency involved in the calculation of curve 1 was corrected by the authors, *i. e.*, in our calculations of curves X and 3, the same value of E_c was used for calculating the exponential factor of the k' as well as for computing Γ_t in B(T).

That is, curves 2 and 3 for both reactions were calculated by using the Eckart I potential, and the E_c of 9.785 and 9.529 kcal/mole were used for curves 2 and 3, respectively. Curves 1, 2 and 3 are compared with experiment in Figure 4. It shows that the consistent curves 2 and 3 deviate considerably from experiment whereas curve 1 agrees with experiment best, but curve 1 includes the inconsistency as pointed out in the above.

In Figure 5, curves 1 and 2 for each reaction of $H+D_2$ and $D+H_2$ were theoretically calculated from Eq. (4) with (5) by the authors by using the CVE potential. In the calculation of curve 1, E_c=9.785 kcal/mole was used for calculating both exponential factor and Γ_t' whereas for calculating curve 2, E_c=9.595 kcal/mole was used for both factors. Figure 5 shows that curve 2 (CVE potential, E_c=9.595 kcal/mole) agrees better with experiment.

5. Discussion

In his paper,[4] Shavitt obtained the "empirical barrier height" E_c=9.785 kcal/mole. He used this value of E_c in his paper since the *ab initio* value of E_c=10.994 kcal/mole obtained by SSMK[17] gives too small values of k's when the latter are calculated from Eq. (4) with (5) and are compared with the experimental k' data of Westenberg and de Haas.[21] Thus he adjusted the *ab initio* E_c so that the theoretical k' calculated from Eq. (4) with (5) coincides with the experimental k' values for the $H+D_2$ and $D+H_2$ reactions at high temperatures, thus he obtained the value of E_c=9.785 kcal/mole. With the latter value, however, the theoretical k' values deviate considerably from experiment at low temperatures. Thus, in computing Γ_t in Eq. (5), he used the Eckart III barrier with E_c=4.005 kcal/mole in order to obtain a complete agreement with experiment (See curves 1 in Figure 4). Our values of E_c=9.595 kcal/mole previously mentioned is slightly less than the Shavitt's values of E_c=9.785 kcal/mole. The latter yields a very good result as shown by curves 1 in Figure 4. As pointed above, however, Shavitt's calculation of curves 1 includes the inconsistency. In addition to the inconsistency,

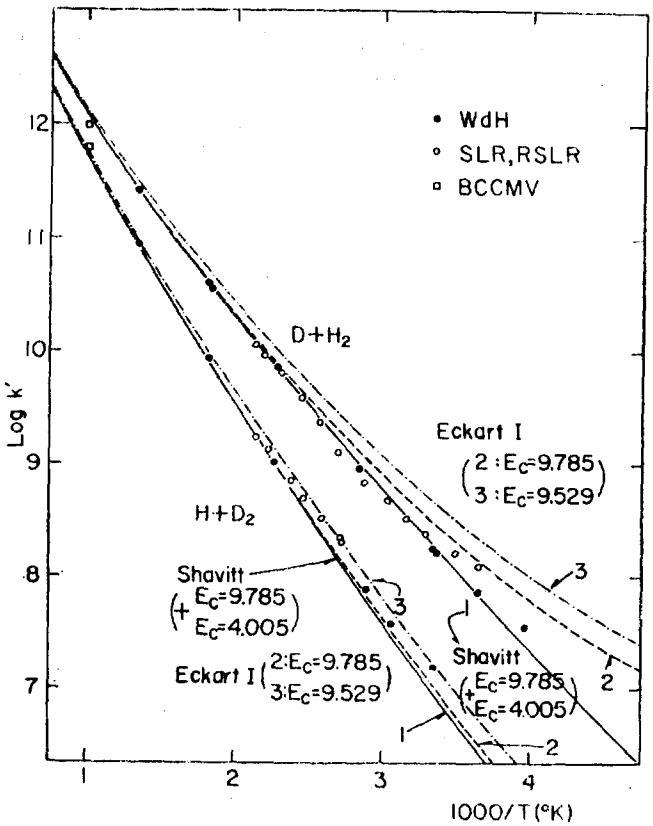

Figure 4. Plots of log k' vs 1000/T for the two reactions of $H+D_2$ and $D+H_2$. Experimental Points: BCCMV (Boato, Careri, Cimino, Molinari and Volpi),[19] SLR (Schultz and Le Roy),[20] WdH (Westenberg and de Haas).[21]
Curve 1. Shavitt curve, E_c=9.785 kcal/mole was used for calculating exp ($-E_c$/RT), E_c=4.005 kcal/mole was used for computing Γ_t; Curves 2 and 3: both were obtained by using Eckart I potential; E_c=9.785 and E_c=9.529 kcal/mole were used for curve 2 and 3, respectively.

the Eckart III barrier yields a contradictory result from experiment as pointed out earlier (see Figure 3). Therefore, the good agreement shown by curves 1, may be due to using the dual values of E_c and also due to the use of an inadequate Eckart III barrier. As previously mentioned, the inconsistency in the Shavitt calculation was corrected in our calculations of curves 2 and 3 in Figure 4, and also pointed out that the theoretically consistent curves 2 and 3 deviate considerably from experiment, especially for $D+H_2$ reaction. This indicates that the Eckart I potential is not suitable for describing the tunnel effect. On the other hand, Figure 5 shows that the CVE potential with E_c=9.595 kcal/mole describes the experimental k' very well for both $D+H_2$ and $H+D_2$ reactions. In connection with this, one may note that the $\Gamma_t \exp\theta_t$ from the CVE potential agrees better with experiment than others (see Figure. 1, 2 and 3). Thus, one may conclude that the rates of $H+D_2$ and $D+H_2$ reactions are described best by activated complex theory with the CVE potential for the tunneling effect.

Tunneling effect has been neglected in most chemical reactions except the reactions involving light atoms like hydrogen atoms. Even in the latter cases, the tunneling effect often has been neglected at high temperatures above 450°K. However,

TABLE 7: Tunnel Factors, Γ_t.

(° K)	$H+H_2$	$D+D_2$	$D+H_2$	$H+D_2$	$T+H_2$	$H+T_2$
150	2886.56	67.300	274.125	955.571	109.364	611.108
200	55.481	7.467	15.063	29.495	9.458	23.677
250	10.650	3.274	4.899	7.270	3.747	6.382
300	4.751	2.201	2.859	3.697	2.402	3.395
350	3.027	1.760	2.116	2.535	1.872	2.388
400	2.292	1.531	1.756	2.009	1.603	1.922
450	1.907	1.395	1.552	1.722	1.446	1.664
500	1.678	1.307	1.423	1.546	1.345	1.504
600	1.425	1.202	1.274	1.348	1.226	1.323
700	1.295	1.144	1.193	1.243	1.160	1.226
800	1.217	1.108	1.144	1.181	1.120	1.168
900	1.167	1.084	1.112	1.140	1.093	1.130
1000	1.133	1.068	1.089	1.111	1.075	1.104
1500	1.057	1.029	1.039	1.048	1.032	1.045
2400	1.022	1.011	1.015	1.018	1.013	1.017

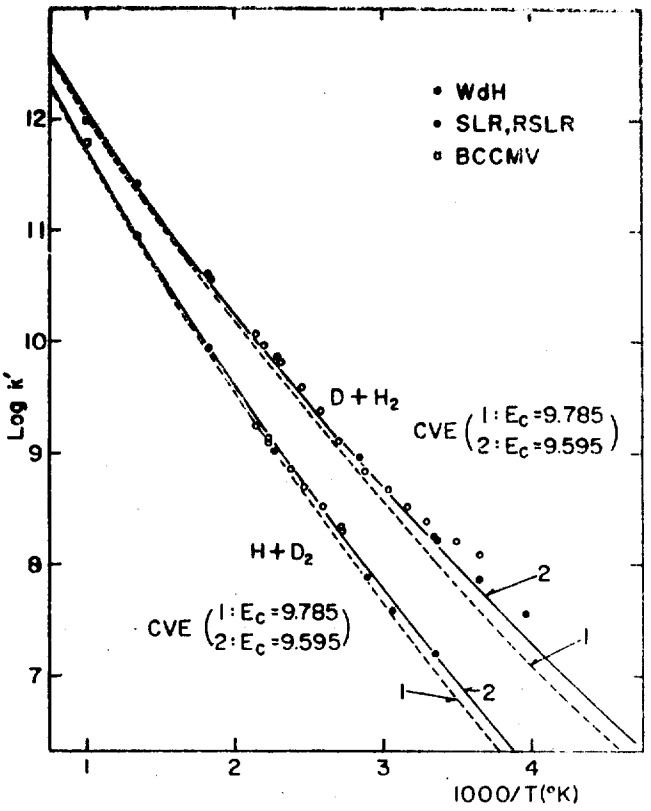

Figure 5. Plots of log k' vs 1000/T for the two reactions of H and $D+H_2$. Experimental Points: refer to the caption to Figure 4. Both curves 1 and 2 were obtained by using the CVE potential, for curve 1 E_c=9.785 kca/mole, for curve 2 E_c=9.595 kcal/mole was used.

according to the theroetical predictions by Garrett and Truhlar[5a] and by Shavitt,[1,4] the tunneling effect is not negligible at temperatures above 450°K for reactions involving hydrogen atoms.

Now, from our results which were calculated from Eq. (12) and are listed in Table 6 (see the second column), we note that the tunneling effect obviously appears at temperatures above 450°K, since the empirical $\Gamma_t \exp\theta_t$ should approach to unity if the tunneling is negligible. The appearance of the tunneling effect at high temperatures is also noticed very easily from Figures. 1 and 2. This fact is different from the prediction by Westenberg and de Haas,[21] who roughly pointed out from their experimental data that the tunneling effect is negligible at temperatures higher than 450° K.

By extending the KAPPAS program for the CVE potential barrier for the $H+D_2$ and $D+H_2$ reactions, the tunneling factor Γ_t for the other isotopic reactions of $H+H_2 \longrightarrow H_2+H$ were calculated, and are tabulated in Table 7. From this Table, one notices that Γ_t converges to unity at about 2400° K for all the isotopic reactions.

Acknowledgement. We are indebted to Dr. Francis H. Ree for providing the KAPPAS program. We also acknowledge the Korea Research Center for Theoretical Physics and Chemistry for a partial support of this work.

References

(1) I. Shavitt, *J. Chem. Phys.*, **31**, 1359 (1959).
(2) H. S. Johnston and D. Rapp, *J. Amer. Chem. Soc.*, **83**, 1 (1961).
(3) H. S. Johnston, "Gas Phase Reaction Rate Theory", Donald Press, New York, 1966, p. 38–47.
(4) I. Shavitt, *J. Chem. Phys.*, **49**, 4048 (1968).
(5) (a) B. C. Garrett and D. G. Truhlar, *J. Phys. Chem.*, **83**, 1079 (1979); (b) **83**, 2921 (1979).
(6) C. Eckart, *Phys. Rev.*, **35**, 1303 (1930).
(7) E. Wigner, *Z. Physik Chem.* (Leipzig), **B19**, 203 (1932).
(8) R. P. Bell, *Trans. Faraday Soc.*, **55**, 1 (1959).
(9) R. A. Marcus, *J. Chem. Phys.*, **46**, 95 (1967).
(10) D. G. Truhlar and A. Kuppermann, *J. Amer. Chem. Soc.*, **93**, 1840 (1971).
(11) R. A. Marcus and M. E. Coltrin, *J. Chem. Phys.*, **67**, 2609 (1977).
(12) B. C. Garrett and D. G. Truhlar, *J. Phys. Chem.*, **83**, 200 (1979).
(13) (a) J. O. Hirschfelder, H. Eyring, and N. Rosen, *J. Chem., Phys.*, **4**, 121 (1936); (b) J. O. Hirschfelder, *ibid.*, **6**, 795 (1938).
(14) G. E. Kimball and J. G. Trulio, *J. Chem. Phys.*, **28**, 493

(1958).
(15) R. N. Porter and M. Karplus, *J. Chem. Phys.*, **40**, 1105 (1964).
(16) H. Conroy and B. L. Bruner, *J. Chem. Phys.*, **42**, 4047 (1965).
(17) I. Shavitt, R. N. Stevens, F. L. Minn and M. Karplus, *J. Chem. Phys.*, **48**, 2700 (1968).
(18) (a) P. Siegbahn and B. Liu, *J. Chem. Phys.*, **68**, 2457 (1978), (b) D. G. Truhlar and C. J. Horowitz, *ibid.* **68**, 2466 (1978).
(19) A. Cimino, E. Molinari, G. Boato, G. Careri, and G. G. Volpi, *J. Chem. Phys.*, **24**, 783 (1956).
(20) (a) W. R. Schultz and D. J. LeRoy, *Can. J. Chem.*, **42**, 2480 (1964); (b) W. R. Schultz and D. J. LeRoy, *J. Chem. Phys.*, **42**, 3869 (1965).
(21) A. A. Westenberg and N. de Haas, *J. Chem. Phys.*, **47**, 1393 (1967).
(22) D. N. Mitchell and D. J. LeRoy, *J. Chem. Phys.*, **58**, 3449 (1973).
(23) R. Weston, Jr. and H. A. Schwarz, "Chemical Kinetics", Prentice-Hall, Inc., Engelwood Cliffs, New Jersey, 1972, p. 95–107.
(24) J. L. Kuester and J. H. Mize, "Optimization Techniques with Fortran," McGraw-Hill, New York, 1973, p. 218–239.
(25) E. W. Schlag, *J. Chem. Phys.*, **38**, 2480 (1963).
(26) V. Gold, *Trans. Faraday Soc.*, **60**, 739 (1964).
(27) E. W. Schlag and G. R. Haller, *J. Chem. Phys.*, **42**, 584 (1965).
(28) D. M. Bishop and K. J. Laidler, *J. Chem. Phys.*, **42**, 1688 (1965).
(29) (a) J. N. Murrell and K. J. Laidler, *Trans. Faraday Soc.*, **64**, 371 (1968); (b) J. N. Murrell and G. L. Prett, *ibid.* **66**, 1680 (1970); (c) D. M. Bishop and K. J. Laidler, *ibid.* **66**, 1685 (1970).
(30) D. R. Coulson, *J. Amer. Chem. Soc.*, **100**, 2992 (1978).

Chain Dimensions and Intrinsic Viscosities of Polypeptides in the Helix–Coil Transition Region

Jong Ryul Kim and Taikyue Ree†

Department of Chemistry, Korea Advanced Institute of Science and Technology, P.O. Box 150, Cheongryangni, Seoul 131, Korea *(Received November 3, 1982)*

An equation is derived which correlates the unperturbed dimensions $\langle r^2\rangle_0$ of polypeptides with the helical contents in the helix-coil transition region by using a simple model of a polypeptide chain. The model is a chain of connected balls which represent the repeating units, -CO-NH-CHR-,based on the fact that the repeating unit has a plane structure. The changing trend of the expansion factor α_η in the transition region is connected with the helical content f_H. The intrinsic viscosities $[\eta]$ of polypeptides are calculated from the unperturbed dimensions and the α_η factors.

The above calculated results concerning $\langle r^2\rangle_0$ and $[\eta]$ are compared with other authors' theoretical and experimental results. From the comparison, we concluded that our theory explains better the chain dimensional behavior of polypeptides in the helix–coil transition region than others.

Introduction

The helical structure of polypeptides was studied early by Pauling *et al.*,[1] the structure was an α–helical structure which includes 3.6 residues or repeating units per turn. Doty *et al.*[2] discovered that polypeptide chains in solution perform a reversible transition between the randomly coiled and the α–helical forms according to the solution conditions. From that time down to this day, experimental researches about the helix–coil transition in polypeptides have been actively under way. For example, there are researches for the effects of solvents,[3] pH[4] and the concentration of a surfactant ion in the solution,[5] and the effects of the temperature and the length of side-chains[6] attached to the polypeptides were also studied. Many researches have been conducted on the conformation of polypeptide molecules by using various kinds of analytical instruments.[7,8]

In theoretical studies, Zimm and Bragg,[9] Lifson and Roig[10] and many others[11] set up the statistical mechanical models for polypeptide molecules. The transformation matrices were individually taken for the three chain elements in one repeating unit –(CO-NH-CHR)–, and then the mean behaviors per three repeating units were calculated. They calculated the helical contents, the sensitivity paramenter of the transition and other properties of polypeptides, *e. g.*, electric moments, relaxation times, *etc.*, But not so many studies were conducted for calculating the chain dimensions in the helix–coil transition region. Nagai[11,12] studied the chain dimensions by applying the Zimm–Bragg theory,[9] But his theoretical results cannot explain the chain dimensional behavior of polypeptides in the transition region, and do not agree with the experimental results even qualitatively.

In order to solve the above difficulty, we set up a new model that is more simple and conclusive than other models. The excluded volume effect on the chain dimensions in the transition region was also studied in this paper, this kind of